

The Bazar shear zone (NW Spain): Microstructural and Time-of-Flight neutron diffraction analysis

Juan Gómez Barreiro, José Ramón Martínez Catalán

Journal of the Virtual Explorer, Electronic Edition, ISSN 1441-8142, volume **41**, paper 5

In: (Eds.) Michele Zucali, Maria Iole Spalla, and Guido Gosso,
Multiscale structures and tectonic trajectories in active margins, 2012.

Download from: <http://virtualexplorer.com.au/article/2011/296/the-bazar-shear-zone-nw-spain>

Click <http://virtualexplorer.com.au/subscribe/> to subscribe to the Journal of the Virtual Explorer.
Email team@virtualexplorer.com.au to contact a member of the Virtual Explorer team.

Copyright is shared by The Virtual Explorer Pty Ltd with authors of individual contributions. Individual authors may use a single figure and/or a table and/or a brief paragraph or two of text in a subsequent work, provided this work is of a scientific nature, and intended for use in a learned journal, book or other peer reviewed publication. Copies of this article may be made in unlimited numbers for use in a classroom, to further education and science. The Virtual Explorer Pty Ltd is a scientific publisher and intends that appropriate professional standards be met in any of its publications.

The Bazar shear zone (NW Spain): Microstructural and Time-of-Flight neutron diffraction analysis

Juan Gómez Barreiro

Departamento de Geología-Geodinámica Interna - Universidad de Salamanca, Spain. *Email: jugb@usal.es*

José Ramón Martínez Catalán

Departamento de Geología-Geodinámica Interna - Universidad de Salamanca, Spain.

Abstract: Unraveling the kinematic and rheological evolution of tectonic contacts it is crucial to understand mass distributions across an orogen. Reactivation of structures is common and might lead to the misunderstanding of the structural evolution. As a consequence, unequivocal determination of the shear sense is required in major contacts. Besides, the interpretation of deformative linear fabrics as transport direction is always a controversial task. The Bazar Shear Zone (BSZ) represents a major regional contact between two allochthonous units in the Ordenes complex (NW Spain), the metagabbroic Monte Castelo unit, with magmatic arc affinities above, and the Bazar ophiolite, below. Previous regional works interpreted the contact as a top-to-the E thrust related to the formation of the Variscan tectonic pile. New crystallographic preferred orientation or texture (TOF-neutron diffraction) and shape fabric data in mylonitic amphibolites suggest that the BSZ recorded a different flow direction, with a top-to-the S shearing. Microstructural analysis suggests a complex interaction of frictional and viscous mechanisms within the shear zone that is compatible with the prevalence of dissolution-precipitation creep. Mechanical and regional implications are discussed.

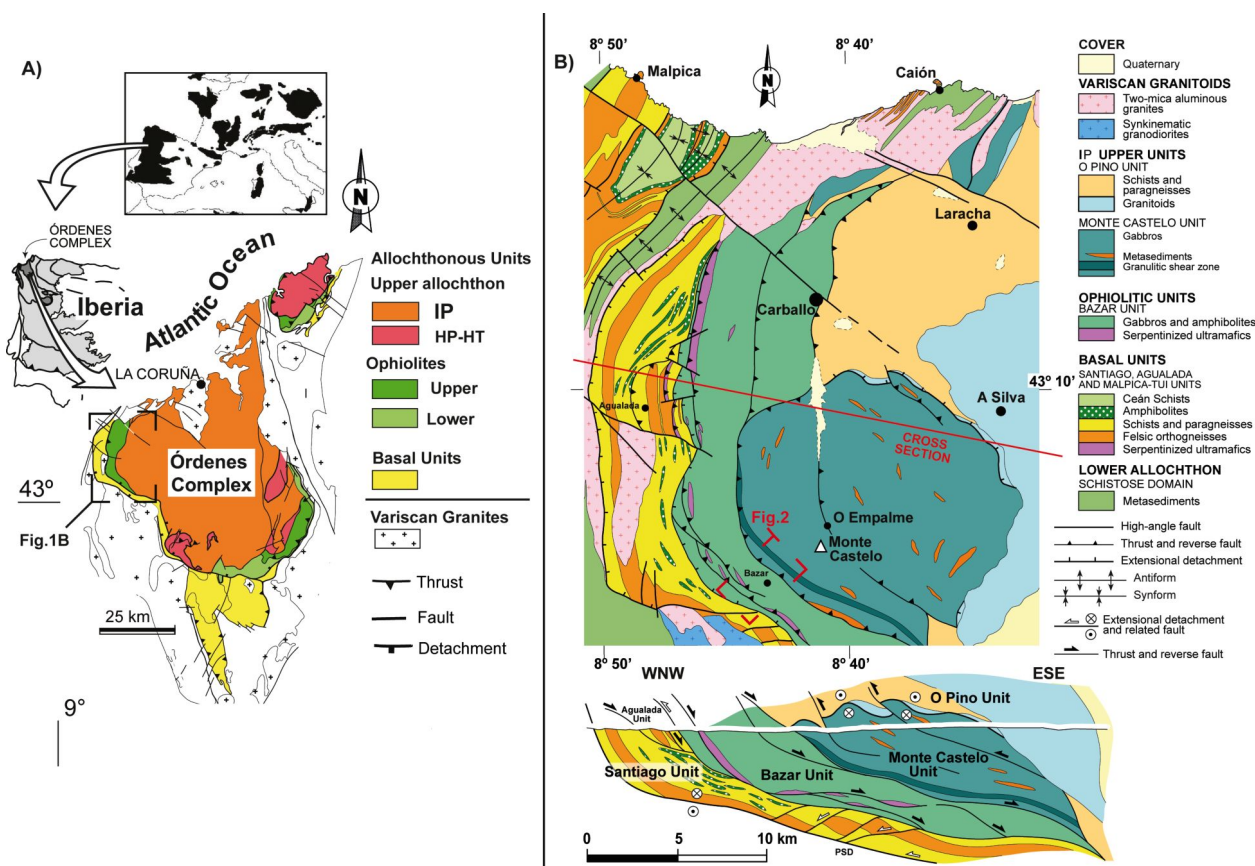
Introduction

Allochthonous units in the NW Iberian Massif

In the NW of the Iberian Massif, an allochthonous nappe stack crops out in five complexes. The Órdenes complex is the largest one, where a complete pile of units can be identified (Gómez Barreiro *et al.*, 2007; Martínez

Catalán *et al.*, 2009). Units have a distinct tectonometamorphic imprint and are separated by tectonic accidents. From bottom to top, in structural order they are: Basal, Ophiolitic, and Upper units, the last one subdivided into High Pressure – High Temperature (HP-HT) units below, and Intermediate – Pressure (IP) units above (Fig. 1 A).

Figure 1. Geology of the Órdenes complex



(A) Geological map of the Órdenes complex and its location in the Iberian Massif (NW Spain). (B) Geological map and representative sections of the NW of the Órdenes complex, where the Bazar ophiolite unit and its relationship with Upper and Basal units are depicted. The inset shows the location of Figure 2. Based on Abati *et al.*, (1999).

Basal units are considered the outermost margin of Gondwana by the time of Variscan orogen (Martínez Catalán *et al.*, 2009). They include terrigenous and metaigneous rocks which recorded the subduction under the accretionary pile during Late Devonian (Abati *et al.*, 2010). The exhumation of the Basal units was driven by ductile eastward thrusting, with the development of regional recumbent folds.

Ophiolitic units represent different oceanic realms existing between the colliding continents Laurussia and Gondwana at that time (Rheic ocean; Arenas *et al.*,

2007). Differences in lithological association, chemical signature and age, led to a subdivision into Upper and Lower ophiolitic units (Fig.1 A; Arenas *et al.* 2007, Sánchez Martínez *et al.* 2009, 2011, and references therein). This assemblage appears tectonically dismembered, and defines the suture of the Variscan orogen in this sector. In some units it is recognized a pre-collisional structure, represented by high-T shear zones with a top-to-the ENE sense of shear, probably initiated in an intraoceanic subductive system, and followed by the building of the accretionary wedge (Díaz García *et al.*, 1999; Gómez

Barreiro *et al.*, 2010a). The emplacement of the suture and overriding units occurs through a system of out-of-sequence thrusts, which led to an imbricate architecture. A top-to-the SE shear sense is commonly associated with this event, but it has not been widely confirmed to a regional scale (Martínez Catalán *et al.* 2002).

Upper units include terrigenous metasediments and metaigneous rocks with arc affinity. HP-HT units consist of paragneisses, basic and ultrabasic metaigneous rocks, metamorphosed under HP granulite to eclogite facies conditions (Martínez Catalán *et al.* 2002; Gómez Barreiro *et al.*, 2006). IP units include terrigenous metasediments and bodies of amphibolites, gabbros and orthogneisses. Metamorphic grade ranges from granulite facies in the lower parts to greenschist facies on top. A polyorogenic evolution is proposed for the Upper units, where several metamorphic cycles and related structures have been identified and dated (Martínez Catalán *et al.*, 2002; Gómez Barreiro *et al.* 2006, 2007a).

The structural evolution of the Variscan suture

Sutures are exceptional witnesses of the orogenesis. Their role as a boundary between colliding continents gives suture units a puzzle nature, and, in many cases, record critical events of pre-collisional and collisional stages (Gómez Barreiro *et al.*, 2010a; Díez Fernández *et al. in press*).

In this paper we are focusing on the Variscan suture that appears in the NW of the Órdenes complex (Fig. 1). In particular we will examine the contentious contact between the IP Upper units and the Ophiolites, named respectively, after local places, the Monte Castelo and Bazar units (Abati, *et al.*, 1999). Regional correlation suggests that this contact could be part of the out-of-sequence thrusts system (Martínez Catalán, 2002). However, reported structural data in the literature indicate a top-to-the E sense of shear (Díaz García, 1990), and may indicate that an older, in-sequence, architecture could be preserved there.

The Bazar ophiolite

The Bazar unit consists of serpentinized ultrabasic and basic metaigneous rocks (gabbros and minor pegmatoid gabbros). The unit represents an N-MORB oceanic lithosphere, probably formed in Late Cambrian times (Sánchez Martínez, 2009). Tectonometamorphic evolution includes: 1) a low/intermediate – pressure granulite-facies

episode, which are preserved in boudins within metabasites, (~7 kbar/ ~700°C; Díaz García, 1990; Sánchez Martínez *et al.*, 2009), and 2) a general retrogression under amphibolite and greenschist facies conditions.

An imbricate structure is recognized, with several slices repeating the basic and ultrabasic association (Díaz García, 1990). Imbrications are limited by faults, in which kinematic criteria are scarce. Those reported in the literature and confirmed in this work suggest a top to the E and NE sense of shear. The main imbrication is located on top of the Bazar unit, and is called the Carballo-Bazar slice. The slice consists of 3500-4000 m of metabasites (amphibolites and flasergabbros) with a foliation developed under HT amphibolite facies conditions (Díaz García, 1990; Sánchez Martínez *et al.*, 2009).

Besides the internal structure of the Bazar ophiolite, the nature of the upper and lower boundaries is controversial. Both limits were soon recognized as tectonic contacts (e.g. Warnars, 1967; Díaz García, 1990). The lower boundary separates the Bazar ophiolite and the Basal units (Díaz García, 1990) and has been interpreted alternatively as an extensional or thrust fault (Gómez Barreiro, 2007b). It has been demonstrated recently that this contact represents a reactivated shear zone, where several extensional detachments overlap previous thrust faults during the gravitational collapse of the Variscan pile (Gómez Barreiro *et al.* 2010b; Díez Fernández *et al.* 2012).

The nature of the upper boundary is unclear. It separates the ophiolite from the base of the IP Upper units above: the Monte Castelo unit (Abati *et al.*, 1999). Different lines of evidence suggest a complex evolution of the tectonic contact. For example, the absence of HP-HT Upper units between the Monte Castelo and Bazar units might be due to a subtractive accident, in the form of an extensional or out-of-sequence low angle shear zone. (Martínez Catalán *et al.*, 2002). However documented kinematic criteria to date are very rare and limited to one observation at the N-S branch of the contact, with an eastward sense of shearing (Díaz García, 1990). New observations along NW-SE branch of the contact are presented below, in order to shed light on the structural evolution of this contact.

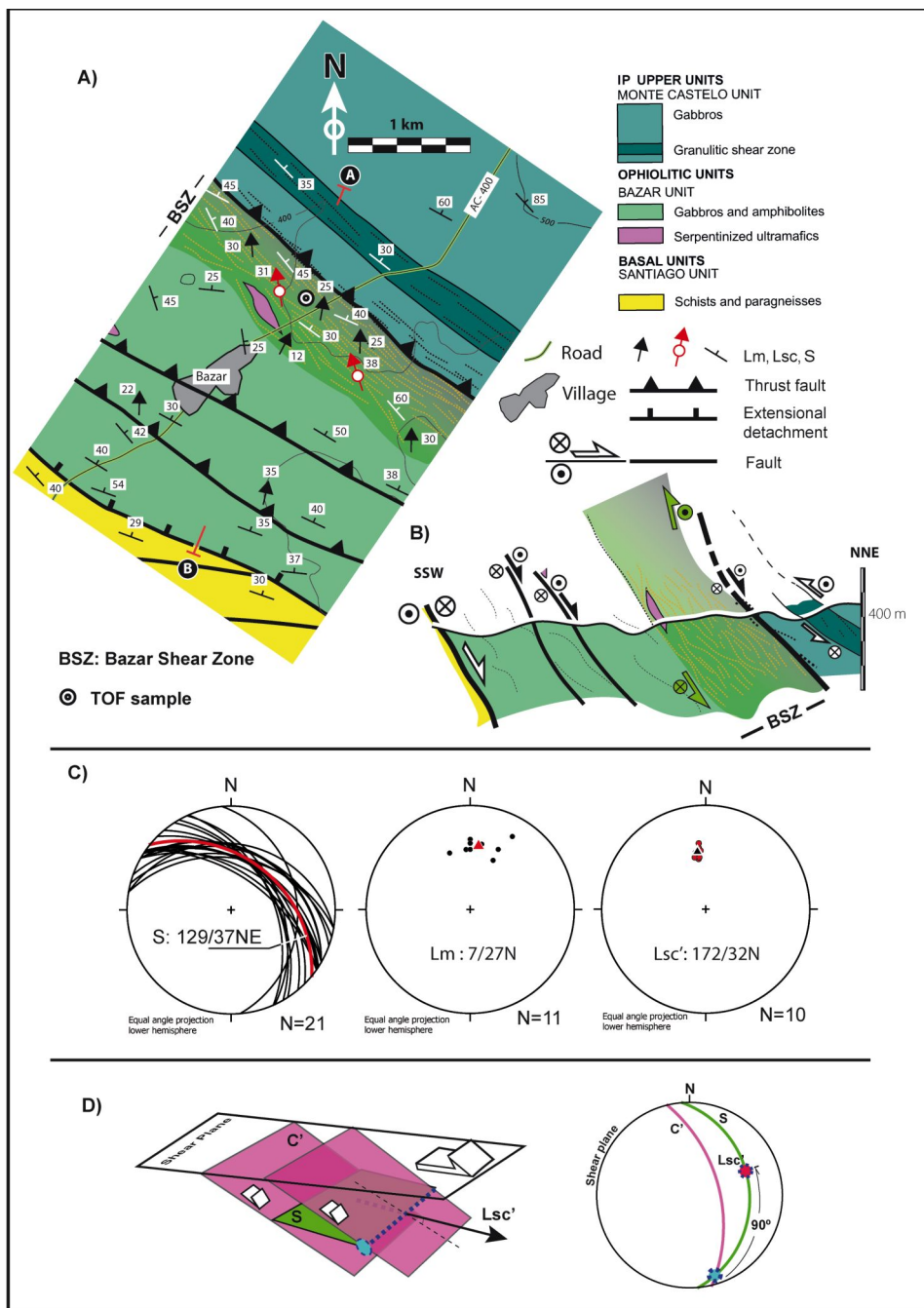
The Bazar shear zone

Structure and kinematics

Along the NW-SE branch of the unit, close to the Bazar village, a new ductile high-strain zone has been identified: The Bazar shear zone (BSZ). The thickness of the shear zone is about 600 m from the contact with the Monte Castelo unit (Fig. 2A, B). Within the shear zone, amphibolites are the most common lithology, but some lenses of phyllonitic metasediments and retrogressed ultramafics have been identified. A penetrative foliation (S_m) and lineation (L_m) are developed across the zone, defined by mineral segregation of amphibole, plagioclase and epidote into fine layers. Preferred orientation of amphiboles define a penetrative linear fabric with a general N-S trend ($L_m = 7/27N$; Fig 2C).

Kinematic criteria are abundant within the shear zone, and show a consistent top - to - the S sense of shear. Shear bands ($SC'C''$), asymmetric folds and σ - porphyroclasts, are common structures (Passchier and Trouw, 1996). We have analyzed shear band fabrics (SC' ; Lister & Snoke 1984; Blenkinsop & Treloar 1995) to obtain flow vectors (LSC'). This is calculated plotting the S- and C'-plane intersection vectors into a stereoplot, and rotating 90° the intersection vectors within the S planes (Fig. 2D; Gómez Barreiro *et al.*, 2010b). Average LSC' flow vector is $172/32N$ (Fig. 2C).

Figure 2. Geological context of the study



(A) Geological map and section (B) of a representative sector of the Bazar shear zone (BSZ). Average fabric (S, Lm, Lsc) data are represented. See the text for a discussion of tectonic contacts. (C) The geometrical calculation of a Lsc' vector is explained (see Gómez Barreiro et al. 2010 for a discussion).

Petrology

There are different types of metabasites in the Bazar shear zone. Mylonitic metabasites are the distinct product of the shear zone. Beside, relics of undeformed or barely deformed metabasites (metagabbros and high temperature amphibolites) could be found at different scales

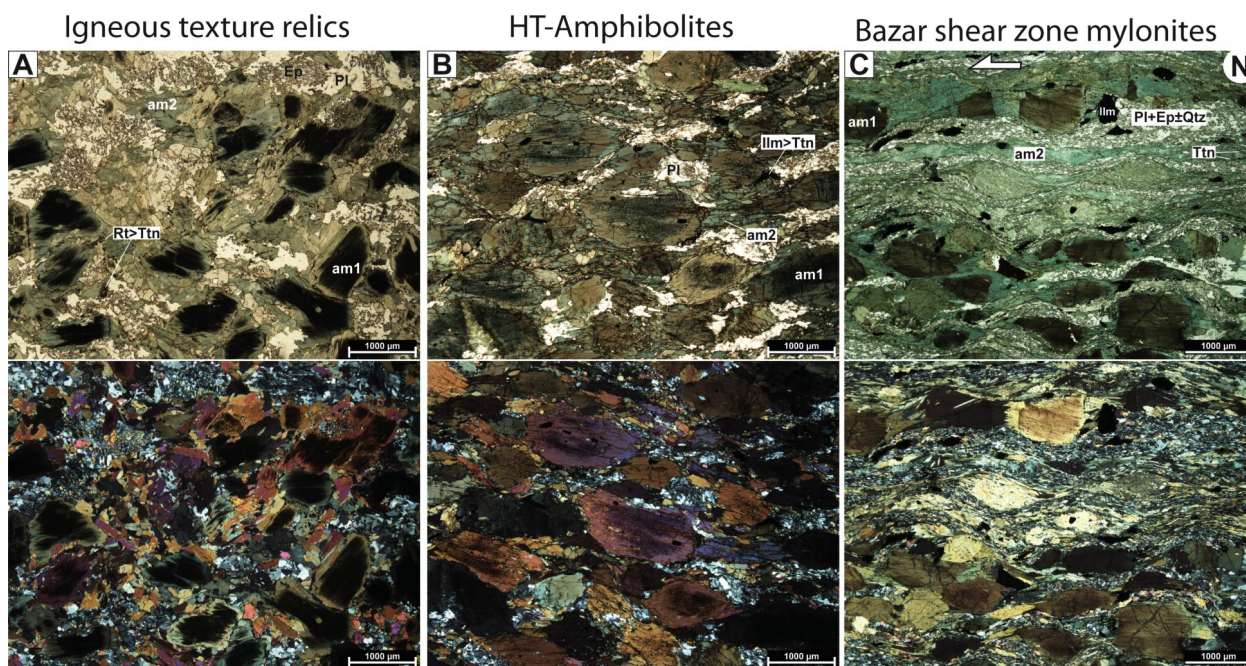
within the mylonites. Those relics correlate well with metabasites types outside the shear zone: Metagabbros and HT-amphibolites.

Undeformed metabasites are more granoblastic, and could preserve gabbroic textures (Fig. 3A, B), mineral abbreviations after Kretz (1983). Brown amphibole

(*am1*), rutile/ilmenite, and plagioclase define the primary mineral assemblage. The *am1* shows cloudy inclusions of opaque minerals, interpreted as Fe-Ti exolutions related to the retrogression of pyroxene (Díaz García, 1990). Apart from igneous relics, plagioclase-amphibole mixtures and load-bearing frameworks are the most common

microstructural configurations in these rocks (LBF, Handy, 1994). Retrogression under the shear zone conditions is also found, with epidote and green/blue amphibole (*am2*) as the main secondary phases defining a rough foliation (Fig. 3B).

Figure 3. Principal metabasite types across the Bazar shear zone



Representative photographs under parallel (upper row) and cross polar (lower row) of principal metabasite types across the Bazar shear zone, including mylonite protholiths (A and B) and mylonites. (A) Metagabbro relics with igneous texture partially preserved are found. Igneous phases are not preserved in these samples, and only amphibolite facies assemblage related to HT event, identified in the Bazar unit, and a partial retrogression under mylonitic conditions are found. (B) HT-amphibolite partially retrogressed under mylonitic conditions, in which a shape fabric is recognized. (C) Mylonites of the Bazar shear zone are characterized by a heterogeneous deformation, with the development of protomylonitic to ultramylonitic fabric. Segregation of phases led to the development of mylonitic layers. Sigmoidal prophyroclasts and C' shear bands show a consistent top-to-the S sense of shear. Porphyroclasts of protholith brown amphibole (*am1*) are preserved in protomylonitic domains, with abundant microcracks, sharp and straight grain boundaries and evidences of dissolution-precipitation creep. Synkinematic blue/green amphibole (*am2*) grows at the strain shadows of *am1* clasts. See the text for a detailed discussion. Abbreviations: *am1* : prekinematic brown amphibole; *am2*: blue/green synkinematic amphibole, Pl: plagioclase, Ilm: ilmenite, Ttn: titanite, Rt: rutile, Ep: epidote, Qtz: quartz.

Mylonitic metabasites depict a strong nematoblastic fabric and segregation of phases into amphibole and plagioclase/epidote – rich layers (Fig. 3C). Most of amphiboles here show a distinct green/blue color (*am2*), and plagioclase appears mixed with epidote grains in the matrix. Ti-phase are ilmenite and titanite which lies along the mylonitic foliation. ilmenite is found as inclusions in titanite grains in the most deformed volumes.

Deformation is highly heterogeneous at all scales. It is commonly observed in mylonitic metabasites the existence of two microstructural domains:

- 1) Protomylonitic domains, where inherited features from undeformed metabasites (Fig. 3 A, B) are preserved, including brownish green amphibole porphyroclasts, and relics of igneous plagioclase porphyroclasts partially transformed into the plagioclase-epidote matrix.
- 2) Mylonitic/ultramylonitic domains show a strong grain-size reduction, where green/blue amphibole (*am2*),

epidote, quartz and plagioclase are the main constituents, typically segregated into compositional bands. Chlorite is scarce and could be located along some shear bands and late microfractures.

Main mineral phases have been identified and characterized in previous works (e.g. Díaz García, 1990). Microprobe analysis of amphibole and plagioclase were recalculated from Díaz García (1990) (Table VII-7), assuming, in the case of amphiboles, total cations equal to 13, except Ca, Na and K (Leake 1978; Spear and Kimball 1984; Leake *et al.* 2004; Yavuz 2007). It is found that amphiboles, *am1* and *am2*, are calcic amphiboles with terms varying among magnesiohastingsite and tschermakite, but pargasite, magnesio-hornblende and edenite terms are also identified. Common plagioclase corresponds to albite (An=3.2%; An % range= 7-0.5%).

We have applied semi-quantitative pressure indicators like the Al content in hornblende (e.g. Anderson and Smith 1995) and Ti in Ca-amphibole (e.g. Ernst & Liu, 1998), that suggests a retrograde trend from *am1* (~7.5 kbar), to *am2* (~6 kbar), and a thermal range between 600° - 500°C (~ 0.67 TiO₂; ~11.85 Al₂O₃). Variation in colour from brown, in *am1* (core), to blue, in *am2* (rim), in prophyroclasts (Fig. 3) could be also related to a reduction in Ti content across the crystal, and hence with a decrease in temperature (e.g. Leake, 1965, Stokes *et al.*, 2012).

After those observations a qualitative evolution of the assemblages could be suggested:

- (1) Ca-rich plagioclase + Ti-rich brown amphibole (*am1*) + rutile/ilmenite + quartz
- (2) albite + Ti-poor blue/green amphibole (*am2*) + epidote + ilmenite/titanite + chlorite + quartz

The evolution from (1) to (2) is coherent with a transition from amphibolite to greenschists facies, in a broad sense (Spear, 1993).

Microstructural analysis

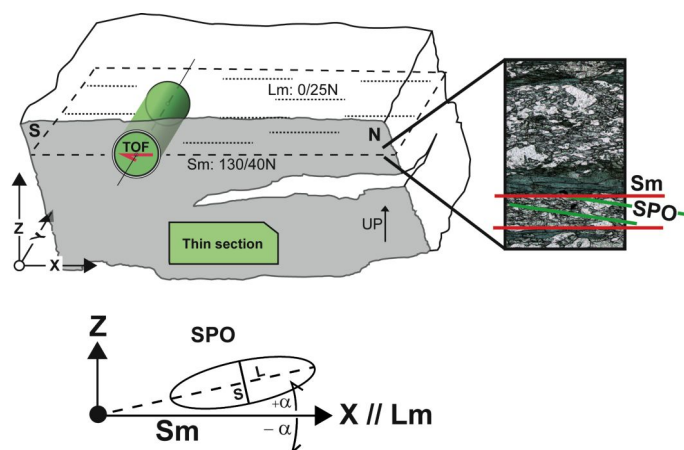
Samples and reference system

In this section the main objective is to characterize the evolution of microstructure across an ideal strain gradient, through the Bazar shear zone. From lower to higher strain we find: a) relics of metagabbros and HT-amphibolites, at different scales and degree of retrogression. They are considered the mylonite protholiths. b) Mylonites, which range from protomylonites to ultramylonites.

Protomylonites correspond to amphibolites with a significant volume of protholith features, particularly, brown amphibole (*am1*). Ultramylonites depict no relics of the protholith.

Observations were carried out with petrographic microscopes on polished rock and thin sections cut perpendicular to the foliation (Sm) and parallel to the lineation (Lm) (XZ plane; Fig. 4). Mylonitic foliation at the outcrop scale correlates with microscopic layering (Sm), defined by alternation of amphibole- and plagioclase- rich mylonitic domains.

Figure 4. Reference system for microstructural and texture analyses



XYZ reference system for microstructural and texture analyses, where X is parallel to the mineral lineation (Lm), and XY to the foliation (Sm). A cylinder parallel to Y and perpendicular to X with a red arrow on top was drilled for TOF texture analysis. A detailed inset shows the fabric elements of an ultramylonitic level. Sm is defined by the compositional layers, being parallel to the shear zone boundary. A shape preferred orientation (SPO) fabric is identified inside each layer, with a monoclinic symmetry, showing a top-to-the S sense of shear. In the lower part, the reference system for SPO analysis is depicted: shape ratio (SR = Long/Short) and orientation ($\alpha = (^\circ)$) is defined by fitting an ellipse to each grain. See the main text for a discussion.

Manually digitized micrographs were analyzed with ImageJ, version 1.4 (W. S. Rasband, U.S. National Institute of Health, <http://rsb.info.nih.gov/ij/>, 1997–2011), and SPO 2003, version 6, software (Launeau and Robin 1996; <http://www.sciences.univ-nantes.fr/geol/UMR6112/SPO>). The grain size (D_{eq}) is defined as the diameter of the equivalent circle with the same area (A) as the measured grain ($D_{eq}^2 = 4A/\pi$; Heilbronner and Bruhn

1998). Selected grain size distributions are plotted using a normalized frequency (F/F_{max} , Fig. 5), but in general, results are presented in parametric form (Table 1).

Table 1: summary of SPO results (part 1)

RELICS OF PRE-SHEAR ZONE FABRICS: METAGABBRO									
	Amphibole 1 (am1)			Amphibole 2 (am2)			Epidote		
	Deq	SR	α	Deq	SR	α	Deq	SR	α
Mean	421.4	2.0	3.9	83.8	2.5	3.5	73.2	2.3	4.6
Median	321.9	1.8	11.0	72.4	2.2	8.2	55.4	2.0	1.7
SD	285.5	1.0	44.8	52.8	1.2	43.1	61.3	1.1	51.4
Kurtosis	0.3	22.1	-0.8	2.4	3.2	-0.8	9.1	2.0	-1.1
Skewness	0.9	4.1	-0.3	1.3	1.6	-0.1	2.5	1.5	-0.1
Minimum	17.4	1.1	-89.8	6.6	1.0	-89.6	6.6	1.0	-89.4
Maximum	1275.2	7.5	83.0	320.3	8.9	87.6	446.9	6.7	90.0
Count	73	73	73	477	477	477	312	312	312

	Plagioclase (igneous)			Plagioclase (recrystallized)			Deq: equivalent diameter (μm)
	Deq	SR	α	Deq	SR	α	
Mean	402.5	1.9	-0.7	79.6	2.0	3.5	SR: shape ratio (long/short)
Median	350.5	1.9	2.0	73.7	1.8	2.6	
SD	170.8	0.7	39.4	47.3	0.8	45.3	α ($^\circ$)
Kurtosis	-0.5	4.5	0.8	19.3	3.0	-0.9	
Skewness	0.6	1.7	-0.1	2.9	1.5	-0.1	
Minimum	126.4	1.1	-88.1	6.6	1.0	-88.5	
Maximum	770.0	4.3	81.2	476.0	6.0	90.0	
Count	31	31	31	261	261	261	

Table 1: summary of SPO results (part 2)

RELICS OF PRE-SHEAR ZONE FABRICS: HT- AMPHIBOLITE						
	Amphibole 1 (am1)			Amphibole 2 (am2)		
	Deq	SR	α	Deq	SR	α
Mean	426.6	2.6	6.1	84.6	3.3	3.9
Median	357.9	2.2	6.0	73.0	2.9	3.2
SD	296.4	1.3	19.1	56.0	1.8	25.5
Kurtosis	1.3	4.9	4.1	6.6	6.1	1.9
Skewness	1.2	2.0	0.6	1.8	1.9	-0.2
Minimum	6.6	1.0	-44.1	6.6	1.0	-88.3
Maximum	1312.5	8.1	87.0	468.2	14.5	85.9
Count	102	102	102	458	458	458

	Plagioclase (recrystallized)			Epidote		
	Deq	SR	α	Deq	SR	α
Mean	51.6	2.2	-6.8	103.2	2.0	6.4
Median	44.3	2.0	-5.9	83.7	2.0	8.5
SD	33.3	0.9	36.2	74.8	0.7	36.9
Kurtosis	6.4	2.3	0.1	2.7	-0.1	-0.7
Skewness	1.8	1.4	0.2	1.6	0.8	-0.1
Minimum	6.5	1.0	-88.3	28.8	1.1	-64.5
Maximum	262.0	6.2	90.0	315.6	3.7	74.1
Count	272	272	272	50	50	50

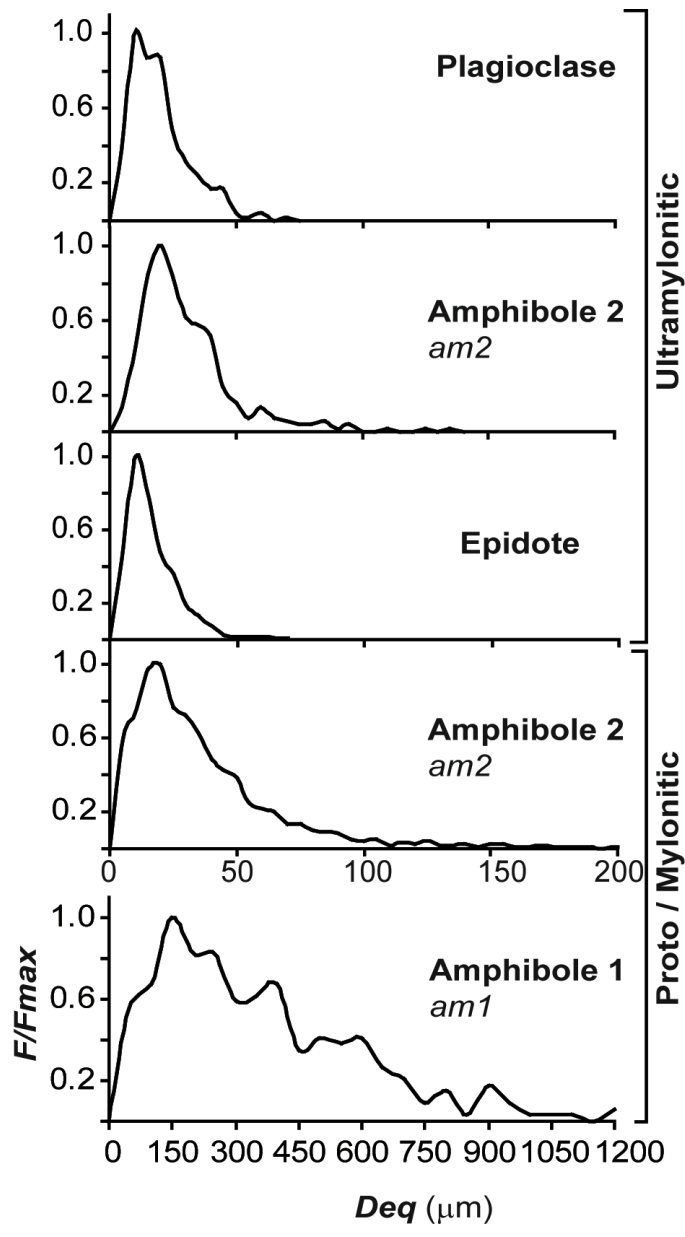
Table 1: summary of SPO results (part 3)

BAZAR SHEAR ZONE FABRIC									
	Amphibole 1 (am1)			Amphibole 2 (am2)			Deq: equivalent diameter (μm)		
	Deq	SR	α	Deq	SR	α			
Mean	334.3	2.0	-2.7	37.8	3.9	-0.3	SR: shape ratio (long/short)		
Median	280.9	1.8	-2.8	26.4	3.2	0.0			
SD	246.4	0.8	34.9	43.6	2.6	25.9	α ($^\circ$)		
Kurtosis	1.0	7.0	0.2	31.6	7.5	1.3			
Skewness	1.1	2.2	0.0	4.5	2.0	0.2			
Minimum	11.7	1.0	-88.9	4.7	1.0	-89.5			
Maximum	1210.7	6.8	85.7	536.0	30.0	90.0			
Count	289	289	289	2118	2118	2118			

ULTRA- MYLONITES									
	Amphibole 2 (am2)			Plagioclase (recrystallized)			Epidote		
	Deq	SR	α	Deq	SR	α	Deq	SR	α
Mean	27.8	7.7	-2.1	17.7	2.9	-3.9	14.8	3.2	-1.8
Median	23.0	6.9	-2.9	15.3	2.7	-1.9	11.8	2.7	-2.3
SD	19.3	4.2	9.4	11.8	1.3	23.1	11.2	1.6	24.5
Kurtosis	5.7	0.2	0.4	1.7	2.1	3.6	7.3	2.9	2.6
Skewness	2.0	0.8	0.5	1.2	1.3	0.1	2.1	1.5	0.1
Minimum	1.3	1.4	-23.9	1.0	1.1	-84.7	0.4	1.0	-89.8
Maximum	133.0	21.7	31.5	69.6	8.9	84.7	92.6	11.9	90.0
Count	312	312	312	245	245	245	743	743	743

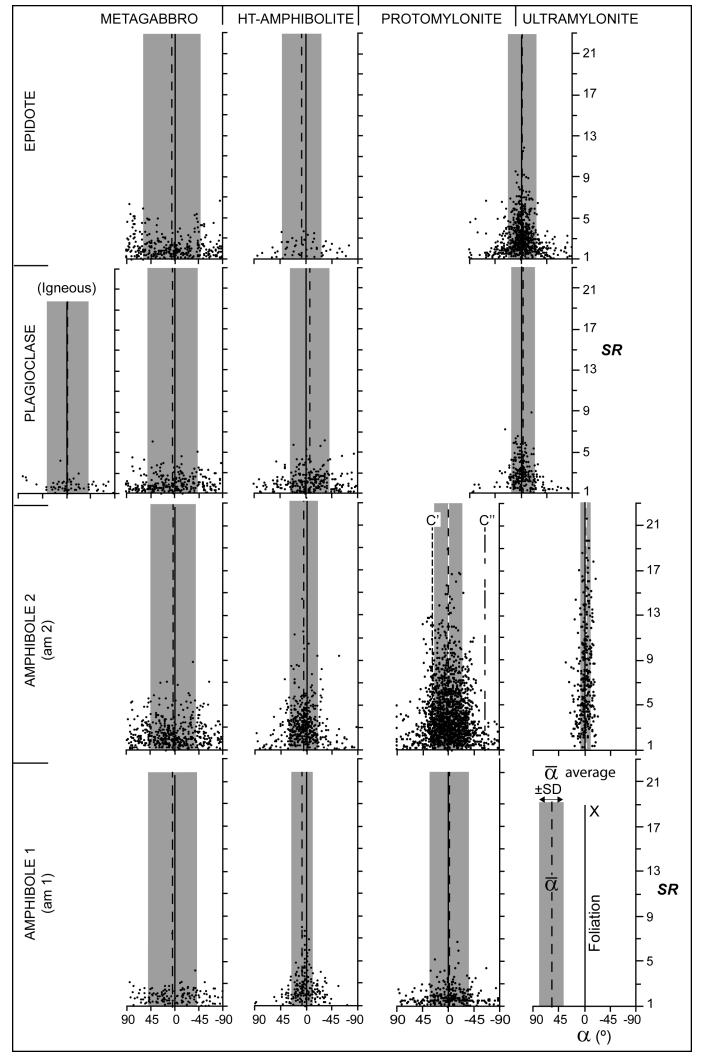
The shape ratio (SR) and the long-axis orientation of each grain (α) are calculated from the inertia tensor of its shape, (Jähne 1991) (Fig. 4). The SR/α graphs were constructed from those data (Fig. 6). Bulk SPOs (SR_p , Φ), were calculated by averaging the inertia tensor of each grain, resulting in an SPO weighted by the area of each grain (Launeau and Cruden 1998). Bulk SPOs were used to correlate different aggregates across the shear zone, and the relative contribution of each rock type to the general fabric (Fig. 7) (Gómez Barreiro *et al.*, 2010a). Microcracks are observed in amphibole porphyroclasts ($am1$) of mylonites, and included in the discussion about deformation mechanisms (Nyman *et al.* 1992; Shelley 1994; Imon *et al.* 2004). Main results of the analysis are presented in Table 1.

Figure 5. Grain size distribution of main phases



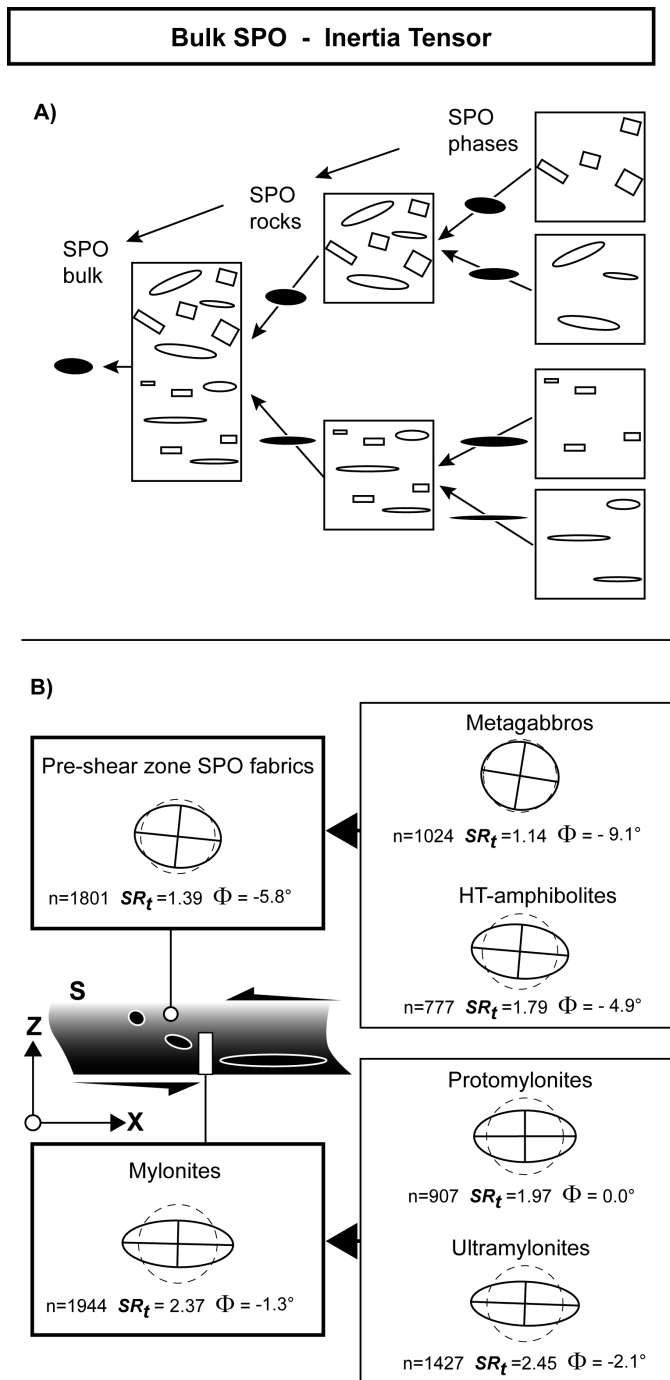
Grain size distribution of main phases in protomylonites/ mylonites and ultramylonites. Normalized frequency (F/Fmax) of the grain equivalent diameter (D_{eq}) is plotted.

Figure 6. SR/ α graphs for main mineral phases and rock types



SR/ α graphs for main mineral phases and rock types. In all cases minerals become more elongated as deformation increase. The dispersion of the grain orientation (SD) is reduced within mylonites, except by amphibole 1 (am1). This is probably explained by the rigid behavior of the am1 grains (porphyroclasts) and the abundance of C'C'' shear bands which deflect the mylonitic foliation. Solid line represents foliation (XY plane; Fig. 4), dashed line, the average grain orientation (α), and the grey bar, the standard deviation (\pm SD) of α (Table 1). The orientation of shear bands C' and C'' are plotted for protomylonites. See the text for a discussion.

Figure 7. Bulk shape preferred orientation



Bulk shape preferred orientation, SPO, (SR_t , Φ), were calculated in different steps by averaging the inertia tensor of each grain, weighted by each area (Launeau and Cruden, 1998). (A) All mineral phases are included, resulting in a mean inertia tensor for each lithology. Digitized grain boundaries were scaled and same area for each rock type combined to build a representation of mylonitic and pre-mylonitic fabric. (B) Metagabbroic rocks show a very weak SPO, while HT-amphibolites define a weak to moderate fabric. Combining both microstructures a bulk SPO for pre-shear

zone fabric is obtained. As explained in the text, some synkinematic phases exist both in metagabbros and HT-amphibolites, so bulk SPO should be interpreted as very low strain rocks within the shear zone (small inset). Mylonites are made of proto to ultramylonites. The combination of those domains results in a strong bulk SPO.

Mylonite protholiths: Metagabbros and HT-amphibolites

The preservation of an igneous texture in metagabbros is distinct and results in a very rough (if any) foliation (Figs 6 and 7B). New phases grew and mimic the old igneous texture, which lead to a bulk random shape fabric ($SR_t=1.14$, $\Phi=-9.1^\circ$). In HT-amphibolites, a foliation is defined ($SR_t=1.79$, $\Phi=-4.9^\circ$) by the preferred orientation of amphiboles (*am1*), and some lensoid domains of recrystallized plagioclase. As a whole, mylonite protholiths depict a low bulk SPO ($SR_t=1.39$; $\Phi=-5.8^\circ$; Fig. 7B) with a monoclinic symmetry that suggests a top-to-the S sense of shear. The contribution of the principal mineral phases is explored below (Fig. 6).

Plagioclase: igneous plagioclases have been completely replaced by polycrystalline aggregates of metamorphic plagioclase and epidote (Fig. 3). Igneous grain shapes are still recognizable, and show mean grain size and shape ratio of $D_{eq} = 402.5 \mu m$ and $SR = 1.9$, respectively. Recrystallized plagioclase results in a drastic grain size reduction, with a mean grain size $D_{eq} = 51.6 - 79.6 \mu m$, for metagabbros and HT-amphibolites. Shape ratio shows no significant variation $SR = 2.0 - 2.2$ (Table 1). All plagioclase grains show a poor preferred orientation ($\alpha \sim 3^\circ \pm 45$; Fig. 6; Table 1). Grains with undulose extinction are common and subgrains are found in larger grains.

Amphibole: Brownish amphibole with inclusions (*am1*) shows a similar grain size than igneous plagioclase, in both rock types ($D_{eq} = 421.4 - 426.6 \mu m$). However, those grains in HT-amphibolites are more elongated ($SR_{HT-amp} = 2.6$ vs $SR_{Metagabbro} = 2.0$), and oriented ($\alpha_{HT-amp} \sim 6^\circ \pm 19$ vs $\alpha_{Metagabbro} \sim 4^\circ \pm 45$; Fig. 6; Table 1). Interestingly blue amphiboles (*am2*) in both rocks present a similar relationship. Scarce undulose extinction and twins are found in both types of amphiboles.

Epidote: epidote crystals have a similar behaviour in metagabbros and HT-amphibolites. Grain size is moderately higher in the second lithology ($D_{eq, Metagabbro} = 73 \mu m$ vs $D_{eq, HT-amp} = 103 \mu m$; Table 1). Shape ratio shows

no significant variation, $SR = 2.0 - 2.3$. Grain orientation presents a similar trend than amphiboles.

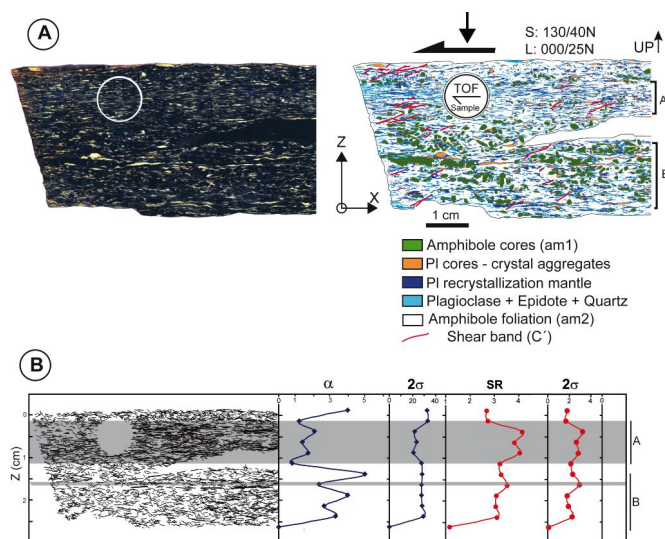
Mylonites

In deformed metabasites the mineral assemblage of microstructural domains are similar, but variation of modal proportion are important, correlating with the progressive deformation of metabasites into the shear zone. Protomylonitic domains appear surrounded by mylonitic and ultramylonitic ones at different scales (Fig. 3).

Shear bands and microdomains

Microdomains in mylonites were analyzed first in polished rock section (XZ) (Fig. 8A). Scanned images were processed into ImageJ in order to perform image segmentation based on gray-levels and colour histograms (e.g. Zucali, 2011). Dark rounded porphyroclasts of amphibole (*am1*), plagioclase porphyroclastic cores, recrystallized mantles, and mixtures of plagioclase, epidote and quartz, were identified within a mass of green amphibole (*am2*) (Fig. 8A). Shear bands show a coherent top-to-the S sense of shear, with the development of two different sets: C' and C'' (Fig. 8 and 9). The presence of $SC'C''$ has been interpreted as developed in stretching shear zones (Passchier, 1991), which means that the shortening direction lies at a relatively high angle to the shear plane, resulting in an effective extension along the flow direction (Passchier and Trouw, 1996).

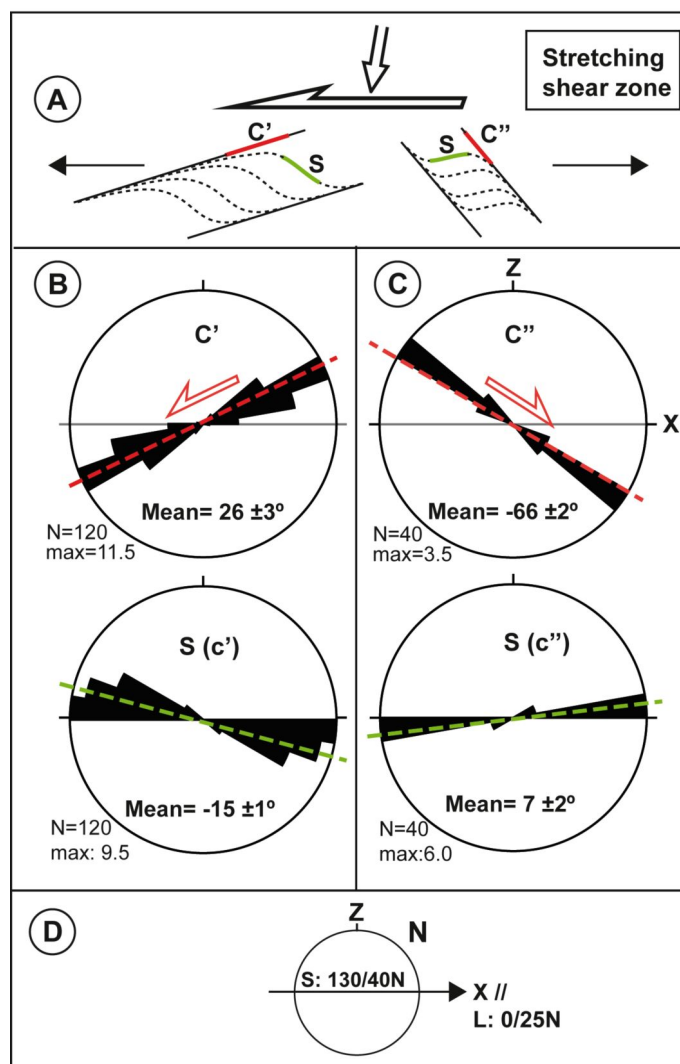
Figure 8. Fabric analysis on polished mylonite sections



Fabric analysis on polished rock sections. An example of common mylonite is presented in (A). Image analysis is used to discriminate different microstructural

domains and major shear bands. Ultramylonitic (A) and protomylonitic (B) layers were analyzed by measuring the shape ratio and orientation (SR, α) of the weakest domains (blue ribbons). B) Spatial projection of the weakest domains results into a distribution of ultramylonitic and protomylonitic layers in the sample (stick bar length is proportional to SR). A correlation between orientation and shape ratio and the dispersion (standard deviation; 2σ), and microstructural domains arise. This analysis was the base for TOF analysis sample preparation.

Figure 9. Shear bands analysis



(A) Development model of $SC'C''$ shear bands in a stretching shear zone (after Passchier and Trouw, 1996). (B) and (C) Rose diagrams of C' and C'' planes in mylonites and corresponding S planes. Results are coherent with a top-to-the S sense of shear. (D) Reference system.

Our results (Fig. 8) demonstrate that the deformation is heterogeneous and two distinct domains are formed at

this scale: A) mylonitic/ultramylonitic ($SR \sim 4$; $\alpha \sim 1.5^\circ \pm 20$) and B) protomylonitic ($SR \sim 3$; $\alpha \sim 4^\circ \pm 30$) (Fig. 8A, B). In ultramylonitic domain (thick grey bands, A; Fig. 8B) highly elongated bands of plagioclase, epidote, and blue amphibole (*am2*) define a strong fabric, while in domain B, porphyroclasts of dark amphibole (*am1*) depict lensoid aggregates, commonly bounded by shear bands ($SC'C''$). The development of synthetic (C') and antithetic (C'') shear bands is coherent with the sense of shearing (Fig. 9).

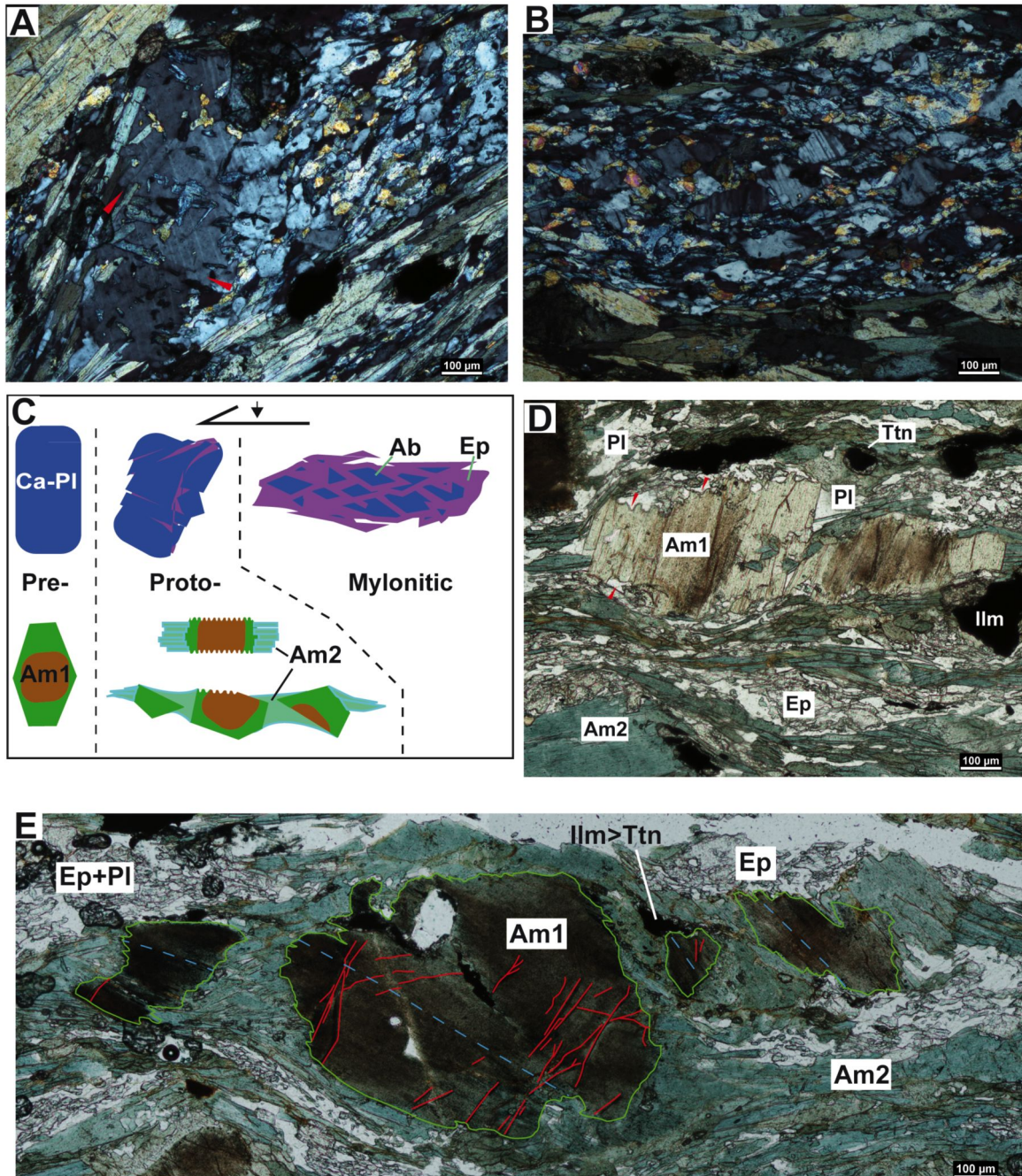
Mylonites

The bulk shape fabric (SR_t ; Φ) of these domains increase from protomylonites to ultramylonites, ($SR_t \sim 1.97 - 2.45$; $\Phi \sim 0^\circ - -2.1^\circ$), and is stronger than bulk SPO in metagabbros and HT-amphibolites. On average SPO's show a monoclinic symmetry for all phases, coherent with a top-to-the S sense of shear, but the angle to the shear plane (Φ , α), is lower than in metagabbros and HT-amphibolites. A typical mylonitic volume would depict a bulk SPO of $SR_t = 2.37$ and $\Phi = -1.3$ (Fig. 7). At the microscopic scale, a grain size reduction between 20 - 80% is confirmed in different phases with respect to the protholiths (Table 1; Fig. 5). Synkinematic phases (amphibole 2, plagioclase and epidote) show a stronger shape fabric as deformation increase (Table 1 and Fig. 6).

In protomylonitic domains, undulose extinction and rare subgrains are found in plagioclase grains. Besides, the shrinkage of plagioclase porphyroclasts (sensu Kenkmann, 2000) into the epidote – plagioclase matrix in mylonitic and ultramylonitic domains is illustrated in Fig. 10A, B, and C. Slightly missoriented domains in a plagioclase porphyroclast in Fig 3A are limited by microcracks. Coeval growth of epidote crystals along those cracks and progressive rotations of fragments led to a complete shrinkage of the clast into the matrix in Fig 3B.

Brown amphibole (*am1*) porphyroclasts show a widespread development of intragrain microcracks (Fig. 3 and 10E). The tensional character of those cracks is recognized elsewhere, with amphibole *am2* growing perpendicular to the crack-wall between the fragments. Moreover, textural zoning in *am1* porphyroclasts are frequently truncated at those faces parallel to the foliation (Fig. 10D). In addition, a preferred growth of blue amphibole (*am2*) prisms occurs at faces perpendicular to the mylonitic foliation (Fig 3 and 10D-E). If we consider the geometry of the system *am1* (core) – *am2* (strain fringes), most grains show a monoclinic symmetry, supporting a top-to-the S shearing, or an orthorhombic symmetry coherent with a stretching component parallel to the mineral lineation (Fig. 3).

Figure 10. Microstructural evidence of solution-transfer creep and brittle mechanisms.



Microstructural evidence of solution transfer creep and brittle mechanisms. (A) Large plagioclase grains in ultramylonitic domains are transformed into a plagioclase + epidote (\pm quartz) matrix by a combination of microcracking (red arrows) and precipitation of other phases (e.g. epidote). (B) Eventually the initial plagioclase porphyroclast is converted in a polycrystalline matrix with a relative misorientation, surrounded by a network of new phases (e.g. epidote, quartz, albite...). (C) Conceptual model of the processes illustrated in A, B, D, and E. (D) Evidence of dissolution-precipitation in amphibole. Truncation of the am1 grain zoning in faces parallel to the foliation. The truncation surface shows a stylolite-like geometry and could be interpreted as a dissolution front (red arrows). Plagioclase and blue amphibole (am2) crystallize in the am1 pressure shadows. (E) Microcracking and solution-precipitation mechanisms in amphibole. Main intragrain cracks are drawn in red. Dashed blue line mark the (hk0) trace.

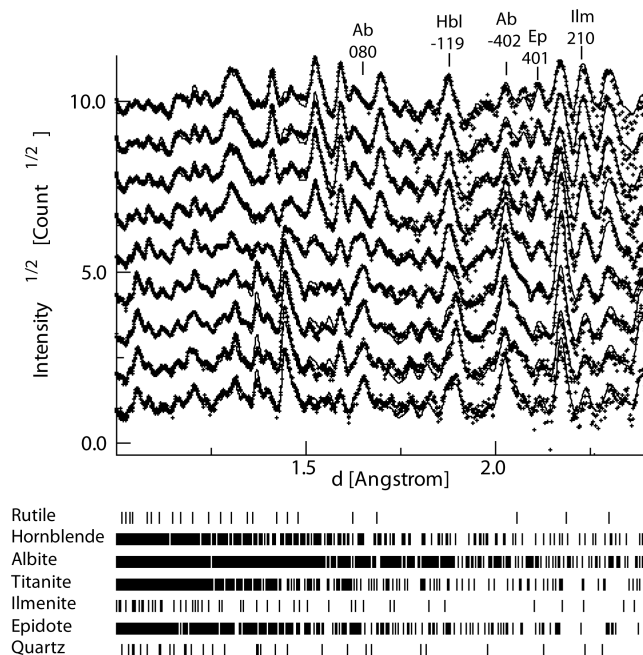
Texture analysis

Texture (crystallographic preferred orientation) measurements were done at HIPPO (High-Pressure Preferred Orientation neutron time-of-flight diffractometer) at Los Alamos Neutron Science Center (LANSCE), New Mexico. Neutrons penetrate deeply into rocks allowing the use of larger samples than other diffraction techniques like EBSD, improving statistics (Xie *et al.*, 2003, Gómez Barreiro *et al.*, 2010A).

Microstructural analysis was crucial to decide the sample selection and orientation. Strain partitioning and severe variation in grain size have to be under consideration, in order to maximize the total number of grains and the homogeneity of the fabric. For those reasons we are focusing on homogeneous levels of ultramylonites, where shear strain is supposed to be most concentrated. Lineation and foliation were also used as a reference system for sample preparation in texture analysis. Oriented cylindrical samples of 10 mm in length and 8 mm in diameter, were drilled perpendicular to the lineation, and parallel to the foliation in order to maximize the volume of ultramylonitic fabric (Fig. 4 and 8)

The oriented cylinder was fully immersed in the neutron beam. For each measurement the sample was rotated around the cylinder axis (perpendicular to the incident neutron beam) into four positions (0°, 45°, 67.5°, 90°) to improve pole figures coverage. The total exposure time was 120 minutes per sample. TOF diffraction spectra, (Fig. 11) were analyzed with the Rietveld method as implemented in the software MAUD (Material Analysis Using diffraction; Lutterotti *et al.* 1999). We use MAUD to extract the orientation distribution function (ODF) from mineral phases, and used it in BEARTEX to calculate and plot pole figures (Wenk *et al.* 1998).

Figure 11. Diffraction spectra for ultramylonitic amphibolite, recorded in HIPPO-neutron diffractometer.



Example of diffraction spectra for ultramylonitic amphibolite, recorded in HIPPO-neutron diffractometer. Relative intensity variations illustrate the presence of texture. Some important peaks are indexed (1st setting, Matthies and Wenk, 2009). Dots represent measured data, and solid lines the results of Rietveld refinement. Peak position for each mineral phase appears at the bottom illustrating the strong overlapping of peaks.

In the Rietveld refinement, crystallographic structures (CIF files) were required. For monoclinic phases, the first setting has to be used, in both MAUD and BEARTEX (Matthies and Wenk, 2009), which requires some transformations. For representations in this article we use labels for second setting (i.e., [010] is the 2-fold axis). It should be noted that due to the low crystal symmetry of major components, for example, hornblende (monoclinic) and plagioclase (triclinic), [100] [010] and [001] directions do not correspond to the pole of the respective crystallographic plane (100) (010) (001), except for [010] in the monoclinic system. Poles of (20-1) (010) (-102) and (-401) (010) (-104) were used as the best approximation to [100] [010] and [001] directions for plagioclase and amphibole, respectively (Xie *et al.* 2003; Gómez Barreiro *et al.* 2007c). In the case of epidote and titanite, poles to (201), (010), (102) and (102), (110), (111) were used respectively. When considering mineral composition and diffraction data, we used hornblende (C/2m) as a general

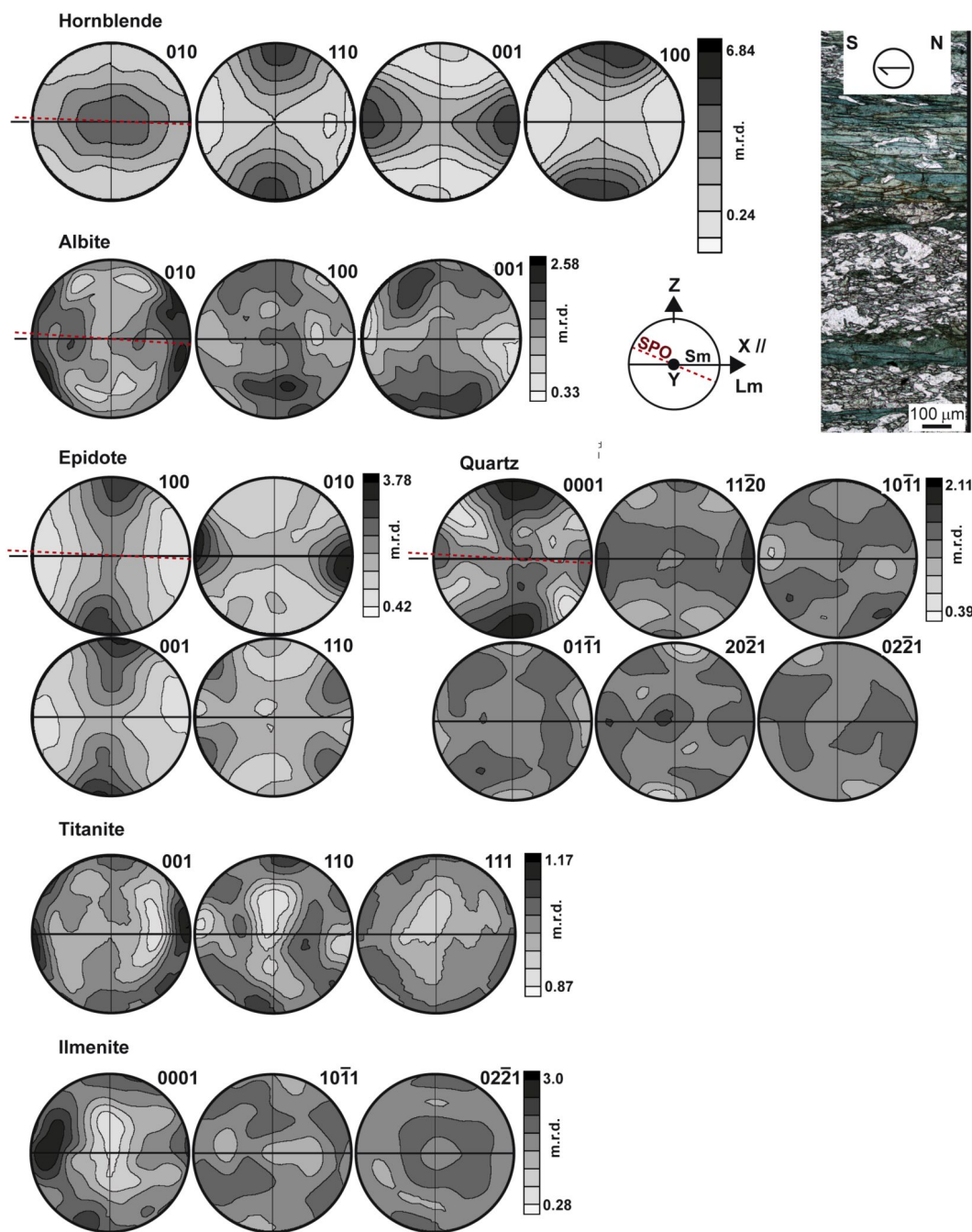
structure for the calcic amphibole, epidote ($P2_1/m$), albite ($P-1$), titanite ($P2$), ilmenite ($R-3$), quartz ($P3_121$) and rutile ($P4_2/mmm$) structures as the starting point for Rietveld analysis (Gómez Barreiro *et al.*, 2010a).

TOF diffraction spectra collected at different angles are showed in Fig. 11. Extreme peak overlapping and variation of relative intensities (Texture) are evident. Volume fraction of each mineral phase was calculated in several thin sections, and refined in MAUD during texture analysis.

Amphibole: In ultramylonitic domains blue/green amphibole (*am2*) is ~ 60% by volume. We use the hornblende structure for calcic amphibole *am2*. Hornblende has a strong crystallographic preferred orientation or texture, with an orthorhombic or slightly monoclinic symmetry, moderate to strong (6.84 m.r.d., multiples of a

random distribution) (Fig. 12). The [001] direction is parallel to the lineation (X) and (100) planes are parallel to the SPO which forms a small angle to the mylonitic foliation (Sm). The [010] direction defines a maximum centered on the Y-axis and elongated along SPO plane. This geometry correlates well with previous studies of amphibole textures (e.g., Gapais and Brun 1981; Siegesmund *et al.* 1989, 1994; Kruhl and Huntemann 1991; Ji and Salisbury 1993; Ji *et al.* 1993; Barroul and Kern 1996; Zucali *et al.*, 2002; Imon *et al.*, 2003; Ivankina *et al.* 2005; Díaz Azpiroz *et al.* 2007; Tatham *et al.* 2008; Gómez Barreiro *et al.* 2010a).

Figure 12. Pole figures from TOF-neutron diffraction analyses of ultramylonitic amphibolite.



Pole figures from TOF-neutron diffraction analyses of ultramylonitic amphibolite sample Equal area projection. Log contours: units in multiples of a random distribution (m.r.d.). Reference system as in Fig. 4.

Plagioclase: Pole figures in albite are complex and depict some degree of monoclinicity. Main features include the cluster of [010] around X-axis (lineation), while [100] and [001] appear projected close to Z-axis (~20-35°; Fig. 12). This phase represents about 14-20% by volume in the ultramylonitic domain.

Epidote: with about 20% volume fraction of the sample, this mineral has a moderate texture (3.78 m.r.d.). Pole figures symmetry are somewhat monoclinic with respect to the mylonitic foliation (Sm). The [010] axis appears parallel to the lineation, while (100), and (001) plot close to the pole of the foliation.

Quartz: this phase is present in about 5-10% in ultramylonitic domains, and shows a weak to moderate texture (2.11 m.r.d.), with basically orthorhombic pole figures, where (0001) poles define a strong maximum parallel to the foliation plane (Z), and a submaximum parallel to the lineation. The (11-20) plane and positive and negative rombs, plot accordingly (Fig. 12)

Titanite and Ilmenite: The volume fraction of these phases is low, but diffraction experiment returned some workable diffraction peaks, resulting in reasonable textures which correlate well with microscopic observations. Preferred orientation of titanite and ilmenite reproduce the orientation of individual grains, with their c-axis parallel to the lineation. A relatively strong minimum in titanite (0.87 m.r.d.) indicates that there is a large number of crystals randomly oriented.

Discussion and conclusions

Regional implications

A high-strain zone has been identified on top of the Bazar ophiolite. Structural and microstructural data demonstrate a general top-to-the S sense of shear. As a consequence, there is no kinetic relationship with those faults that bound the internal imbricates of the Bazar unit, which present a general top-to-the N and NE sense of shear (e.g. Díaz García, 1990). The limited number of outcrops prevented us to find cross-cutting relationships between those accidents, so the presented results alone cannot decipher the structural sequence. However, regional evidences in other units of the allochthonous complexes suggest a sequence of W-E-directed thrust system followed by a SE-directed out-of-sequence thrust system (Martínez Catalán *et al.*, 2002). These include another ophiolitic unit (Careón unit; Díaz García *et al.* 1999; Gómez Barreiro *et al.*, 2010a), the Upper units (Gómez Barreiro *et al.*, 2007a), and some sectors of the the Basal units (Gómez Barreiro, *et al.*, 2010b; Díez Fernández *et al.* 2012).

As a regional conclusion, we suggest that the Bazar Shear zone represents a part of the out-of-sequence thrust system which carried the Ophiolitic units and the Upper allochthon over the Basal allochthon and Parautochthon (Martínez Catalán *et al.*, 2009). The meaning of the NE kinematics found within the Bazar unit will be examined in a future work, but they could be related to the in-sequence thrust system, identified in other sectors of the

allochthonous complexes (Díez Fernández and Martínez Catalán, 2012)

Deformation conditions and mechanisms

Across the deformation gradient in the Bazar shear zone, distinct metamorphic changes occur. The relation between mineral phases and microstructures suggests that reactions were synkinematic with the activity of the Bazar shear zone. While more quantitative and extense work is needed, we could speculate about the qualitative meaning of those changes. Petrographic and previous chemical data suggest a retrogressive evolution from amphibolite facies to greenschist facies conditions. We are aware about the upscaling limitation, a common problem when extrapolation from small scale experiments to nature is pursued. In consequence our results should be considered preliminary.

Microstructural analysis reveals a brittle behaviour in pre-kinematic amphibole (brown amphibole *am1*) (Fig. 10), but not in synkinematic phases (*am2*, epidote albite). This is supported by the abundance of intragrain microcracks and the fragmentary character (sharp boundaries, “domino-like”) of most *am1* porphyroclasts. On the other hand grain size distribution with a low frequency of large grains and a high frequency of small ones is coherent with the activity of cataclastic processes (Passchier and Trouw, 1996).

These features are not present in metabasites outside the shear zone, and are found in an incipient stage of development in relics of HT-amphibolites located across the shear zone. Apparently synkinematic phases accommodate this behaviour by ductile deformation, which include the envelope of *am1* clasts by mylonitic and ultramylonitic layers, and the filling of gaps between the *am1* fragments with *am2* fibres. Those fibers sometimes track the separation of the fragments or simply depict a normal angular relation to crack planes and envelope *am1*-rich domains (protomylonitic) with continuous mylonitic/ultramylonitic layers.

Moreover, truncation of *am1* porphyroclasts mineral zoning, in those faces parallel to the foliation, and development of *am2* strain fringers in the opposite faces is a common feature in these mylonites. These findings could be interpreted as the removal of amphibole *am1* by dissolution, along crystal faces perpendicular to the shortening direction (foliation plane), and precipitation of synkinematic amphibole *am2*, parallel to the tensile direction

(mineral lineation). These observations have been interpreted to reflect stress-induced grain-boundary diffusive mass-transfer or pressure solution (Durney, 1972; Robin, 1978; Raj, 1982; Lehner, 1990; Wheeler, 1992, Whinch and Yi, 2002).

The dissolution-precipitation creep is an effective mechanism to develop (or amplify) shape fabric (SPO), and, potentially, crystallographic preferred orientation or texture (e.g. Hippertt, 1994; Stallard and Shelley, 1995; Bons and den Brok, 2000; Stokes *et al.*, 2012). Growth and dissolution rates are anisotropic in many minerals. Growth is faster along c-axis in amphibole and quartz (Anh *et al.*, 1991; Stallard and Shelley, 1995). The role of the brittle mechanisms documented in these mylonites could be important at the initial stages of deformation, by reducing the grain-size of the phases and increasing the grain boundary surface in the aggregate (Table 1, Fig. 10). All these features are compatible with the presence of a fluid phase, which promotes also synkinematic metamorphic reactions, at the grain boundary network. The combination of those processes as a cooperative group, in the deformation of metabasites, has already been proposed in the literature (e.g. Brodie and Rutter, 1985; Nyman *et al.* 1992; Lafrance and Vernon, 1993; Berger and Stünitz, 1996; Imon *et al.*, 2004).

Complementary information comes from texture in the ultramylonitic domains (Fig. 12). The limited evidence of intracrystalline plasticity suggests that other mechanisms could be accounting for the strain accommodation in the matrix. The symmetry of pole figures reflects, to some extent, the combination of rotational and non-rotational components of the flow. In the case of amphibole (*am2*), pole figure patterns are compatible with the activity of the main slip system (100) [001] (Biermann and Van Roermund, 1983; Biermann, 1981; Skrotzki, 1992). However, an equivalent texture could be developed by rigid rotation of grains and/or slip on (110) cleavage plane, in a general context of dissolution-precipitation creep (e.g. Allison and La Tour, 1977; Babaie and La Tour, 1994). The strongly anisotropic crystal growth of amphibole may result in grains with very high shape ratios (*SR*) that tend to rotate toward a stable end orientation, close to the attractors of the fabric (lineation and foliation; Passchier, 1997, Mancktelow *et al.*, 2002), resulting in a strong texture.

Albite, epidote and quartz appear typically segregated in a different layer than amphibole (Fig. 12). Diffusive

mass-transfer could explain some observations, such as the shrinkage of larger plagioclase crystals into the epidote-plagioclase matrix (Fig. 10). However, the presence of some evidence of intracrystalline plasticity, points to the activation of some other mechanisms in these domains. Interestingly, texture of albite shows a very uncommon pattern, with (010) poles parallel to the lineation and [100] and [001] plotting close to the foliation pole. To our knowledge, [010] has never been identified as a slip direction in plagioclase (Gómez Barreiro *et al.*, 2007c, 2010a, and references therein). Some similarities could be drawing with textures obtained by Heidelberg *et al.* (2000), after experimentally deformed fine-grained albite aggregates by solution precipitation creep. They found a strong texture, with the (010) poles tending to lie orthogonally to the compression direction. Another supporting argument comes from crystal-growth experiments and observations in nature, where the [010]-axis is generally considered the faster growth direction for plagioclase (e.g.: Muncill and Lasaga, 1987, Deer *et al.*, 1967). In summary we suggest that the albite texture could be interpreted as the result of solution precipitation creep.

The measurement of epidote texture is not common in fabric studies. Our results are slightly monoclinic, and depict pole figure patterns similar to those reported in mid-low grade mylonites (Crampton, 1957), blueschists (Bezacier *et al.*, 2010), and eclogites (Cao *et al.* 2011), with (010) poles parallel to the lineation and (001) (100) parallel to the foliation. There is an incomplete knowledge of epidote slip systems (e.g. Din *et al.*, 2001). Bezacier *et al.* (2010) suggest that [010] has the shortest Burgers vectors, so it could be the easy slip direction in epidote. As a consequence, our textures could be interpreted as the result of dislocation glide on [010] (001) (100). However we cannot exclude other mechanisms as rigid rotation of grains as an alternative way to develop such a texture.

As a summary, deformation in the Bazar shear zone is likely to have occurred under amphibolite to greenschists facies conditions. Microstructures suggest a combination of simple and pure shear (stretching shear) dominating the flow. In addition, shape and crystallographic fabrics are compatible with the activity of several mechanisms such as cataclasis, solution transfer, passive rotation, and, to some extent, intracrystalline strain. While not necessarily coeval processes, brittle and ductile mechanisms, accounted for the strain accommodation in the rock,

reflecting the mechanical contrast among phases like amphibole and plagioclase. The existence of a distinct texture in plagioclase developed under dissolution-precipitation creep is supported by our results. There is strong evidence about the importance of solution transfer creep transfer in mid-crust (wet) shear zones (e.g. Wincht and Yi, 2002; Stokes et al, 2012). Whether this mechanism dominated or not along a major tectonic contact like the Bazar shear zone, must be carefully evaluated if a proper rheological evolution is to be drawn.

Acknowledgements

This work has been funded by research project CGL2011-22728 of the Dirección General de Programas

y Transferencia del Conocimiento (Spanish Ministry of Science and Innovation), as part of the National Program of Projects in Fundamental Research, in the frame of the VI National Plan of Scientific Research, Development and Technologic Innovation 2008-2011. JGB appreciates financial support by the Spanish Ministry of Science and Innovation through the Ramón y Cajal program. Access to LANSCE (HIPPO) to perform texture measurements, and help of Sven Vogel was invaluable. We are grateful to M. Voltolini and M. Zucali for thorough and constructive reviews and to M. Zucali for the editorial work and the invitation to participate in this volume.

References

- Abati, J., Dunning, G.R., Arenas, R., Díaz García, F., González Cuadra, P., and Martínez Catalán, J.R., 1999, Early Ordovician orogenic event in Galicia (NW Spain): Evidence from U-Pb ages in the uppermost unit of the Ordenes Complex, Earth Planet. Sc. Lett., 165: 213-228. 10.1016/S0012-821X(98)00268-4
- Abati, J., Gerdes, A., Fernández-Suárez, J., Arenas, R., Whitehouse, M. J., Díez Fernández, R., 2010. Magmatism and early-Variscan continental subduction in the northern Gondwana margin recorded in zircons from the basal units of Galicia, NW Spain. GSA Bull., 122: 219-235. 10.1130/B26572.1
- Ahn, J.H., Moonsup C., Jenkins, D.M., Buseck, P.R., 1991, Structural defects in synthetic tremolitic amphiboles, Am. Mineral., 76: 1811-1823.
- Allison, I. and La Tour, T.E., 1977, Brittle deformation of hornblende in a mylonite: a direct geometrical analogue of ductile deformation by translation gliding. Can. J. Earth Sci., 14, 1953-1958.
- Anderson, J.L. and Smith, D.R., 1995, The effects of temperature and fO_2 on the Al-in-hornblende barometer. Am. Mineral., 80: 549-559.
- Arenas, R., Martínez Catalán, J.R., Sánchez Martínez, S., Díaz García, F., Abati, J., Fernández-Suárez, J., Andonaegui, P., and Gómez-Barreiro, J., 2007, Paleozoic ophiolites in the Variscan suture of Galicia (northwest Spain): Distribution, characteristics, and meaning, in 4-D Framework of Continental Crust edited by R.D., Jr., Hatcher, M.P. Carlson, J.H. McBride and J.R. Martínez Catalán. Geol. Soc. Am. Mem. 200: 425-444
- Babaie, H.A., and La Tour, T.E., 1994. Semibrittle and cataclastic deformation of hornblende-quartz rocks in a ductile shear zone. Tectonophysics, 229: 19-30. 10.1016/0040-1951(94)90003-5
- Barroul, G., and Kern, H. 1996. Seismic anisotropy and shear-wave splitting in lower-crustal and uppermantle rocks from the Ivrea Zone: experimental and calculated data. Phys. Earth Planet. Inter. 95:175-194. 10.1016/0031-9201(95)03124-3
- Berger, A., and Stünitz, H., 1996, Deformation mechanisms and reaction of hornblende: examples from the Bergell tonalite (Central Alps), Tectonophysics, 257: 149-174. 10.1016/0040-1951(95)00125-5
- Bezacier, L. Reynard, B., Bass, J.D., Wang, J., and Mainprice, D., 2010, Elasticity of glaucophane, seismic velocities and anisotropy of the subducted oceanic crust. Tectonophysics 494:, 201-210.
- Biermann, C. 1981, (100) deformation twins in naturally deformed amphiboles. Nature, 292:821-823. 10.1038/292821a0
- Biermann, C., and H. L. M. Van Roermund. 1983. Defect structures in naturally deformed clinoamphiboles: a TEM study. Tectonophysics, 95: 267-278. 10.1016/0040-1951(83)90072-0
- Blenkinsop, T.G. and Treloar, P.J. 1995. Geometry, classification and kinematics of S-C and S-C' fabrics in the Mushandike area, Zimbabwe. J. Struct. Geol., 17: 397-408. 10.1016/0191-8141(94)00063-6
- Bons, P. D., and den Brok, B. W. J. 2000. Crystallographic preferred orientation development by dissolution precipitation creep. J. Struct. Geol. 22: 1713-1722. 10.1016/S0191-8141(00)00075-4
- Brodie, K.H. and Rutter, E., 1985. On the relationship between deformation and metamorphism, with special reference to the behavior of basic rocks. In: A.B. Thompson and D.C. Rubie (Editors), Metamorphic Reactions: Kinetics, Texture and Deformation. Adv. Phys. Geochem., 4: 138-179.
- Cao, Y., Song, S.G., Niu, Y.L., Jung, H., and Jin, Z.M., 2011, Variation of mineral composition, fabric and oxygen fugacity from massive to foliated eclogites during exhumation of subducted ocean crust in the North Qilian suture zone, NW China, J. metamorphic Geol., 29: 699-720.
- Crampton, C. B., 1957, Regional study of epidote, mica, and albite fabrics of the Moines. Geol. Mag., 94, 89-102. 10.1017/S0016756800068370
- Deer, W.A., Howie, R.A, and Zussman, J., 1967. An introduction to the rock-forming minerals. Longman, London, England.
- Díaz Azpiroz, M., Lloyd, G.E., Fernández, C. 2007. Development of lattice preferred orientation in clinoamphiboles deformed under low-pressure metamorphic conditions – A SEM/EBSD study of metabasites from the Aracena metamorphic belt, SW Spain. J. Struct. Geol., 29: 62-645.
- Díaz García, F., 1990, La Geología del sector Occidental del Complejo de Órdenes (Cordillera Hercínica, Noroeste de España), Nova Terra, 3, 289 pp.
- Díaz García, F., Arenas, R., Martínez Catalán, J. R., González del Tánago, J., and Dunning, G. R., 1999. Tectonic evolution of the Careón Ophiolite (northwest Spain): a remnant of oceanic lithosphere in the Variscan Belt. J. Geol. 107:587-605. 10.1086/314368
- Díez Fernández, R., Foster, D.A., Gómez Barreiro, J., and Alonso-García, M., (accepted). Rheological control on the tectonic evolution of a continental suture zone: the Variscan example from NW Iberia (Spain), Int. J. Earth Sci.
- Díez Fernández R, Martínez Catalán JR, Gómez Barreiro J, Arenas R, 2012. Extensional flow during gravitational collapse: a tool for setting plate convergence (Padrón migmatitic dome, Variscan belt, NW Iberia). J. Geol., 120: 83-103.

- Díez Fernández, R. and Martínez Catalán, J. R., 2012. Stretching lineations in high-pressure belts: the fingerprint of subduction and subsequent events (Malpica–Tui complex, NW Iberia) *J. Geol. Soc. London*, 169: 531–543.
- Din, S.U., Ahamd, M. and Chishti, S., 2001. Study of Slip Systems in Epidote Single Crystal. *Turk. J. Phys.*, 25: 229–235.
- Dollinger, G. and Blacic, J.D., 1975. Deformation mechanisms in experimentally and naturally deformed amphiboles. *Earth Planet. Sc. Lett.*, 26: 409–416. 10.1016/0012-821X(75)90016-3
- Durney, D.W., 1972, Solution-transfer, an important geological deformation mechanism. *Nature*, 235: 315–317. 10.1038/235315a0
- Ernst, W.G. and Liu, J., 1998, Experimental phase-equilibrium study of Al- and Ti-contents of calcic amphibole in MORB—A semiquantitative thermobarometer, *Am. Mineral.*, 83: 952–969.
- Gapais, D., and Brun, J.-P. 1981. A comparison of mineral grain fabrics and finite strain in amphibolites from eastern Finland. *Can. J. Earth Sci.*, 18: 995–1003. 10.1139/e81-095
- Gómez Barreiro, J.; Wijbrans, J. R.; Castiñeiras, P.; Martínez Catalán, J. R.; Arenas, R.; Díaz García, F.; and Abati, J., 2006, 40Ar/39Ar laserprobe dating of mylonitic fabrics in a polyorogenic terrane of the NW Iberia. *J. Geol. Soc. London.*, 163: 61–73. 10.1144/0016-764905-012
- Gómez Barreiro, J., J.R. Martínez Catalán, R. Arenas, P. Castiñeiras, J. Abati, F. Díaz García and Wijbrans, J.R. 2007a. Tectonic evolution of the upper allochthon of the Órdenes complex (northwestern Iberian Massif): Structural constraints to a polyorogenic peri-Gondwanan terrane. In U. Linnemann, R.D. Nance, P. Kraft and G. Zulauf eds. *The evolution of the Rheic Ocean: From Avalonian-Cadomian active margin to Alleghenian-Variscan collision*. *Geol. Soc. Am. Spec. Paper*, 423: 315–332.
- Gómez Barreiro, J. 2007b. La Unidad de Fornás: Evolución tectonometamórfica del SO del Complejo de Órdenes. *Laboratorio Xeológico de Laxe, Serie Nova Terra*, 32, 291 pp.
- Gómez Barreiro, J., I. Lonardelli, H.-R. Wenk, G. Dresen, E. Rybacki, Y. Ren and C.N. Tomé, 2007c. Preferred orientation of anorthite deformed experimentally in Newtonian creep. *Earth Planet. Sc. Lett.*, 264: 188–207. 10.1016/j.epsl.2007.09.018
- Gómez Barreiro, J., Martínez Catalán, Prior, D., Wenk, H.-R., Vogel, S., Díaz García, F., Arenas, R., Sánchez Martínez, S., and Lonardelli, I., 2010^a. Fabric development in a Middle Devonian intra-oceanic subduction regime: the Careón ophiolite (NW Spain). *J. Geol.*, 118: 163–186.
- Gómez Barreiro, J., Martínez Catalán, J.R., Díez Fernández, R., Arenas, R., Díaz García, F., 2010b. Upper crust reworking during gravitational collapse: The Bembibre-Pico Sacro detachment system (NW Iberia). *J. Geol. Soc. London*, 167: 769–784. 10.1144/0016-76492009-160
- Handy, M.R., 1994, Flow laws for rocks containing two nonlinear viscous phases: A phenomenological approach, *J. Struct. Geol.*, 16: 287–301, Correction, 1994, *J. Struct. Geol.*, 16: 12, 1727.
- Heidelbach, P., Post, A., and Tullis, J., 2000. Crystallographic preferred orientation in albite samples deformed experimentally by dislocation and solution precipitation creep, *J. J. Struct. Geol.*, 22: 1649–1661. 10.1016/S0191-8141(00)00072-9
- Heilbronner, R., and D. Bruhn 1998. The influence of three-dimensional grain size distributions on the rheology of polyphase rocks. *J. Struct. Geol.*, 20: 695–705. 10.1016/S0191-8141(98)00010-8
- Hippertt, J.F., 1994. Microstructures and c-axis fabrics indicative of quartz dissolution in sheared quartzites and phyllonites. *Tectonophysics*, 229: 141–163. 10.1016/0040-1951(94)90026-4
- Huang, X.G., Bai, W.M. and Hu, J.M., 2003. Experimental studies on elastic and rheological properties of amphibolites at high pressure and high temperature. *Science in China Series D-Earth Sciences*, 46: 1212–1222.
- Imon, R., Okudaira, T., Fujimoto, A., 2002. Dissolution and precipitation processes in the deformed amphibolites: an example from the ductile shear zone of the Ryoke metamorphic belt, SW Japan. *J. Metamorph. Geol.*, 20: 297–308. 10.1046/j.1525-1314.2002.00367.x
- Imon, R.; Okudaira, T.; and Kanagawa, K., 2004. Development of shape- and lattice-preferred orientations of amphibole grains during cataclastic deformation and subsequent deformation by dissolution-precipitation creep in amphibolites from the Ryoke metamorphic belt, SW Japan. *J. Struct. Geol.*, 26:793–805. 10.1016/j.jsg.2003.09.004
- Ivankina, T.I., Kern, H.M. and Nikitin, A.N., 2005. Directional dependence of P- and S-wave propagation and polarization in foliated rocks from the Kola superdeep well: Evidence from laboratory measurements and calculations based on TOF neutron diffraction. *Tectonophysics*, 407: 25–42. 10.1016/j.tecto.2005.05.029
- Jähne, B. 1991. *Digital image processing, concepts, algorithms and scientific applications*. New York, Springer.
- Ji, S., and Salisbury, M. H. 1993. Shear-wave velocities, anisotropy and splitting in high-grade mylonites. *Tectonophysics*, 221: 453–473. 10.1016/0040-1951(93)90173-H
- Ji, S.; Salisbury, M. H.; and Hammer, S. 1993. Petrofabric, P-wave anisotropy and seismic reflectivity of high-grade tectonites. *Tectonophysics*, 222: 195–226. 10.1016/0040-1951(93)90049-P
- Kenkmann, T. 2000, Processes controlling the shrinkage of porphyroclasts in gabbroic shear zones. *J. Struct. Geol.* 22: 471–487. 10.1016/S0191-8141(99)00177-7

- Kretz, R., 1983, Symbols for rock-forming minerals. *Am. Mineral.*, 68: 277-279
- Kruhl, J. H., and Huntemann, T., 1991. The structural state of the former lower continental crust in Calabria (S. Italy). *Geol. Rundsch.*, 81: 289-302. 10.1007/BF01829367
- Lafrance, B. and Vernon, R.H., 1993. Mass transfer and microfracturing in gabbroic mylonites of the Guadalupe igneous complex, California. In: J.N. Boland and J.D. Fitz Gerald (Editors), *Defects and Processes in the Solid State: Geoscience Applications. Dev. Petrol.*, 14: 151-167.
- Launeau, P., and Cruden, A. R., 1998. Magmatic fabric acquisition mechanisms in a syenite: results of a combined anisotropy of magnetic susceptibility and image analysis study. *J. Geophys. Res.*, 103: 5067-5089. 10.1029/97JB02670
- Launeau, P., and Robin, P.-Y. F. 1996. Fabric analysis using the intercept method. *Tectonophysics* 267: 91-119. 10.1016/S0040-1951(96)00091-1
- Leake, B.E., 1965. The relationship between composition of calciferous amphiboles and grade of metamorphism. In: *Controls of Metamorphism. W.S. Pitcher and G.W. Flinn, Eds.*, 299-318. London, Oliver and Boyd.
- Leake, B. E., 1978. Nomenclature of amphiboles. *Am. Mineral.*, 63: 1023-1052.
- Leake, B. E.; Woolley, A. R.; Birch, W. D.; Burke, E. A. J.; Ferraris, G.; Grice, J. D.; Hawthorne, F. C., et al. 2004. Nomenclature of amphiboles: additions and revisions to the International Mineralogical Association's amphibole nomenclature. *Am. Mineral.*, 89: 883- 887.
- Lehner, F.K., 1990. Thermodynamics of rock deformation by pressure solution. In: Barber, D.J., Meredith, P.D. (Eds.), *Deformation Processes in Minerals, Ceramics and Rocks. Unwin Hyman, London*, pp. 296-333. 10.1007/978-94-011-6827-4_12
- Lister, G.S. and Snoke, A.W. 1984. S-C Mylonites. *J. Struct. Geol.*, 6: 617-638. 10.1016/0191-8141(84)90001-4
- Lutterotti, L.; Matthies, S.; and Wenk, H.-R. 1999. MAUD: a friendly Java program for materials analysis using diffraction. *Int. Union Crystallogr. Comm. Powder Diffr. News.*, 21: 14 -15.638.
- Mancktelow, N.S., Arbaret, L., and Pennachioni, G., 2002, Rotational behaviour of rigid particles in simple shear: experimental and natural observations on stabilization due to interface slip, *J. Struct. Geol.*, 24: 567-585. 10.1016/S0191-8141(01)00084-0
- Martínez Catalán, J. R., Díaz García, F., Arenas, R., Abati, J., Castiñeiras, P., González Cuadra, P., Gómez Barreiro, J., and Rubio Pascual, F., 2002. Thrust and detachment systems in the Ordenes Complex (northwestern Spain): implications for the Variscan- Appalachian geodynamics. In Martínez Catalán, J. R., Hatcher, R. D., Jr., Arenas, R., and Díaz García, F., eds. *Variscan-Appalachian dynamics: the building of the Late Paleozoic basement. Geol. Soc. Am. Spec. Pap.*, 364: 163-182.
- Martínez Catalán, J.R., Arenas, R., Abati, J., Sánchez Martínez, S., Díaz García, F., Fernández Suárez, J., González Cuadra, P., Castiñeiras, P., Gómez Barreiro, J., Díez Montes, A., González Clavijo, E., Rubio Pascual, F.J., Andonaegui, P., Jeffries, T.E., Alcock, E., Díez Fernández, R., and López Carmona, A., 2009, A Rootless Suture and the Lost Roots of a Mountain Chain: The Variscan Belt of NW Iberia, *Comptes Rendus Geosciences*, 341: 114-126. 10.1016/j.crte.2008.11.004
- Matthies, S., and Wenk, H.-R. 2009. Transformations for monoclinic crystal symmetry in texture analysis. *J. Appl. Cryst.*, 42:564-571. 10.1107/S0021889809018172
- Muncill, G.E., and Lasaga, A.C., 1987. Crystal-growth kinetics of plagioclase in igneous systems: One-atmosphere experiments and application of a simplified growth model. *Am. Mineral.*, 72: 299-311.
- Nyman, M.W., Law, R.D. and Smelik, E.A., 1992. Cataclastic deformation for the development of core mantle structures in amphibole. *Geology*, 20: 455-458. 10.1130/0091-7613(1992)020<0455:CDMFTD>2.3.CO;2
- Passchier, C.W., 1991. Geometric constraints on the development of shear bands in rocks. *Geol. Mijnb.*, 70: 203-211.
- Passchier, C.W., 1997. The fabric attractor, *J. Struct. Geol.*, 19: 113-127. 10.1016/S0191-8141(96)00077-6
- Passchier, C.W. and Trow, R.A.J. 1996. *Microtectonics. Springer, Berlin*, 289 pp.
- Raj, R., 1982. Creep in polycrystalline aggregates by matter transport through a liquid phase. *J. Geophys. Res.*, 87: 4731 4739. 10.1029/JB087IB06p04731
- Robin, P.Y., 1978. Pressure solution at grain-to-grain contacts. *Geochim. Cosmochim. Acta*, 42: 1383-1389. 10.1016/0016-7037(78)90043-1
- Sánchez Martínez, S., Arenas, R., Fernández-Suárez, J. and Jeffries, T.E., 2009, From Rodinia to Pangaea: ophiolites from NW Iberia as witness for a long-lived continental margin. In: Murphy, J.B., Keppie, J.D. and Hynes, A.J. (eds) *Ancient Orogens and Modern Analogues. Geol. Soc. London, Spec. Pub.*, 327: 317-341.

- Sánchez Martínez, S., Arenas, R., Gerdes, A., Castiñeiras, P., Potrel, A., Fernández Suárez, J., 2011, Isotope geochemistry and revised geochronology of the Purrido Ophiolite (Cabo Ortegal Complex, NW Iberian Massif): Devonian magmatism with mixed sources and involved Mesoproterozoic basement. *J. Geol. Soc. London*, 168: 733-750. 10.1144/0016-76492010-065
- Shelley, D., 1994. Spider texture and amphibole preferred orientation. *J. Struct. Geol.*, 16: 709-717. 10.1016/0191-8141(94)90120-1
- Siegesmund, S.; Helmig, K.; and Kruse, R. 1994. Complete texture analysis of a deformed amphibolite: comparison between neutron diffraction and U-stage data. *J. Struct. Geol.*, 16: 131-142. 10.1016/0191-8141(94)90024-8
- Siegesmund, S.; Takeshita, T.; and Kern, H. 1989. Anisotropy of Vp and Vs in an amphibolite of the deeper crust and its relationship to the mineralogical microstructural and textural characteristics of the rock. *Tectonophysics*, 157: 25-38. 10.1016/0040-1951(89)90338-7
- Skrotzki, W. 1992. Defect structures and deformation mechanisms in naturally deformed hornblende. *Phys. Status Solidi*, 131: 605-624. 10.1002/pssa.2211310232
- Spear, F.S., 1993, *Metamorphic Phase Equilibria and Pressure-Temperature-Time Paths*, 799 p. Mineralogical Society of America, Washington, D. C.
- Spear, F. S., and Kimball, K. L. 1984. RECAMP: a Fortran IV program for estimating Fe 3+ contents in amphiboles. *Comp. Geosci.* 10: 317-325. 10.1016/0098-3004(84)90029-3
- Stallard, A., and Shelley, D., 1995, Quartz c-axes parallel to stretching directions in very low-grade metamorphic rocks, *Tectonophysics*, 249: 31-40. 10.1016/0040-1951(95)00040-T
- Stokes, M.R., Wintsch, R.P. and Southworth, C. S., 2012, Deformation of amphibolites via dissolution-precipitation creep in the middle and lower crust. *J. Metamorphic Geol.*, 30: 723-737. 10.1111/j.1525-1314.2012.00989.x
- Tatham, D.J., Lloyd, G.E., Butler, R.W.H., Casey, M. 2008. Amphibole and lower crustal seismic properties. *Earth Planet. Sci. Lett.*, 267: 118-128. 10.1016/j.epsl.2007.11.042
- Warnaars, F.W., 1967, Petrography of a peridotite amphibolite and gabbro bearing polyorogenic terrain NW of Santiago de Compostela (Spain). *Leidse Geologische Mededelingen*, 36.
- Wenk, H.-R.; Matthies, S.; Donovan, J.; and Chateigner, D. 1998. BEARTEX: a Windows-based program system for quantitative texture analysis. *J. Appl. Cryst.*, 31: 262-269. 10.1107/S002188989700811X
- Wenk, H.-R., Lutterotti, L., Vogel, S.C., 2010, Rietveld texture analysis from TOF neutron diffraction data. *Powder Diffraction*, 25: 283-296 10.1154/1.3479004
- Wheeler, J., 1992. Importance of pressure solution and coble creep in the deformation of polymineralic rocks. *J. Geophys. Res.*, 97: 4579-4586. 10.1029/91JB02476
- Wintsch, R.P. and Yi, K., 2002. Dissolution and replacement creep: a significant deformation mechanism in mid-crustal rocks. *J. Struct. Geol.*, 24: 1179-1193. 10.1016/S0191-8141(01)00100-6
- Xie, Y.; Wenk, H.-R.; and Matthies, S. 2003. Plagioclase preferred orientation by TOF neutron diffraction and SEM-EBSD. *Tectonophysics*, 370: 269-286. 10.1016/S0040-1951(03)00191-4
- Yavuz, F. 2007. WinAmphcal: a windows program for the IMA-04 amphibole classification. *Geochem. Geophys. Geosyst.*, 8: 1-12. 10.1029/2006GC001391
- Zucali, M., Chateigner, D., Dugnani, M., Lutterotti, L., and Ouladdiaf, B. 2002. Quantitative texture analysis of glaucophanite deformed under eclogites facies conditions (Sesia-Lanzo Zone, Western Alps): comparison between X-ray and neutron diffraction analysis. In: de Meer, S., Drury, M.R., de Bresser, J.H.P. and Pennock, G.M. (eds.), *Deformation mechanisms, Rheology and Tectonics: Current Status and Future Perspectives*. Geological Society, London, Spec. Pub., 200: 239-253.
- Zucali, M., (2011), Coronitic microstructures in patchy eclogitised continental crust: the Lago della Vecchia pre-Alpine metagranite (Sesia-Lanzo Zone, Western Italian Alps), *J. Virt. Explor.*, Electronic Edition, ISSN 1441-8142, volume 38, paper 5 In: (Eds.) M.A. Forster and J.D. Fitz Gerald, *The Science of Microstructure - Part II*.